Article ID: 1006-8775(2017) 02-0121-12

LOW–DEFORMATION VORTICITY AREAS IN SYNOPTIC–SCALE DISTURBANCES FOR TROPICAL CYCLOGENESIS: AN OBSERVATIONAL ANALYSIS

DUAN Jing-jing (段晶晶)[1, 2], WU Li-guang (吴立广)[1, 3]
(1. Pacific Typhoon Research Center and Key Laboratory of Meteorological Disaster of Ministry of Education, University of Information Science and Technology, Nanjing 210044 China; 2. Ningbo Meteorological Observatory of Zhejiang Province, Ningbo 315012 China; 3. State Key Laboratory of Severe Weather, Chinese Academy of Meteorological Sciences, Beijing 100029 China)

Abstract: It has long been known that incipient tropical cyclones (TCs) always occur in synoptic-scale disturbances or tropical cyclogenesis precursors, and the disturbances can intensify only within a limited area during tropical cyclogenesis. An observational analysis of five tropical cyclogenesis events over the western North Pacific during 11 August to 10 September 2004 is conducted to demonstrate the role of synoptic-scale disturbances in establishing a limited area of low-deformation vorticity for tropical cyclogenesis.

The analysis of the five tropical cyclogenesis events shows that synoptic-scale tropical cyclogenesis precursors provide a region of low-deformation vorticity, which is measured with large positive values of the Okubo-Weiss (OW) parameter. The OW concentrated areas are within the tropical cyclogenesis precursors with a radius of about 400-500 km and can be found as early as 72 hours prior to the formation of the tropical depression. When the TCs reached the tropical storm intensity, the concentrated OW is confined to an area of 200-300 radius and the storm centers are coincident with the centers of the maximum OW. This study indicates that the tropical cyclogenesis occurs in the low-deformation 18-72 hours prior to the formation of tropical depressions, suggesting the importance of low-deformation vorticity in pre-existent synoptic-scale disturbances. Although the Rossby radius of deformation is reduced in TC genesis precedes, the reduction does not sufficiently make effective conversion of convective heating into kinetic energy within the low-deformation area. Further analysis indicates that the initial development of four of the five disturbances is coupled with the counterclockwise circulation of the mixed Rossby-Gravity (MRG) wave.

Key words: synoptic-scale disturbances; low-deformation vorticity; Okubo-Weiss parameter; Rossby radius of deformation

CLC number: P444 **Document code:** A

doi: 10.16555/j.1006-8775.2017.02.001

1 INTRODUCTION

Tropical cyclogenesis can be taken as a process for the construction of a self-sustaining warm-cored cyclonic vortex in which multi-scale interactions are involved. While it has long been known that tropical cyclogenesis always occurs in the area of pre-existent synoptic-scale disturbances or so-called tropical cyclogenesis precursors (Riehll[1]; Ramage[2]; Ooyama[3]; Zehr[4]; Gray[5]), which can be observed at low-levels as a synoptic-scale(~700 km), organized but weak wind field with multiple mesoscale convective systems (Gray [5]), a recent marsupial concept provides new insights into the influence of tropical cyclogenesis precursors on tropical cyclogenesis (Dunkerton et al.[6]; Wang et al.[7]; Montgomery et al. [8]; Montgomery et al. [9]). In this framework, tropical cyclogenesis precursors play an important role in the establishment of the marsupial pouch, a closed gyre favorable for tropical cyclogenesis. Although the parent synoptic-scale system in the marsupial concept was originally proposed for easterly waves, Wang et al. [10] and Tory et al. [11] recently suggested that the framework can provide useful guidance on early tropical cyclogenesis detection.

In the WNP, the monsoon trough in the low troposphere has been identified as one of the important large-scale circulation patterns that provide necessary large-scale conditions favorable for tropical cyclogenesis (Sadler[12-13]; Gray[14-15]; Frank[16]; Chen et al.[17, 18]). Tropical disturbances in the monsoon trough are often associated with northwest-propagating wave trains on the synoptic time scale, which are characterized by alternating regions of cyclonic and anticyclonic circulations along

Received 2015-04-20; **Revised** 2017-03-29; **Accepted** 2017-05-15

Foundation item: National Natural Science Foundation of Ningbo (2016A610208); National Basic Research Program of China (2013CB430103, 2015CB452803); National Natural Science Foundation of China (41275093); project of the specially-appointed professorship of Jiangsu Province

Biography: DUAN Jing-jing, Ph. D., primarily undertaking research on numerical simulation and tropical cyclones.

Corresponding author: WU Li-guang, e-mail: liguang@nuist.edu.cn

the trough line (e. g., Nitta[19]; Lau and Lau[20]; Takayabu and Nitta [21]; Chang et al.[22]; Sobel and Bretherton[23]). Previous studies on the roles of tropical cyclogenesis precursors were mainly focused on the differences in temperature, moisture, low-level vorticity and vertical motion between developing and non-developing disturbances (Zehr[24]; McBride and Zehr[25]; Lee[26]; Fu et al. [27]). While larger low-level vorticity and stronger vertical motion were identified in developing cloud clusters, these studies found little difference in temperature and moisture between developing and non-developing disturbances.

Dunkerton et al. proposed a new pathway for TC formation within a tropical easterly wave and suggested that the synoptic wave plays a vital role in establishing a quasi-closed region of recirculating horizontal flow that protects from hostile exterior influences (i.e., dry air intrusion and shear/strain deformation) [6]. In the easterly wave, the preferred location for tropical cyclogenesis or the pouch center can be identified as the intersection of the trough axis and the critical layer. Wang et al.[28, 29] and Montgomery et al.[30] showed that the marsupial pouch provides a focal point for the merger of vortical convective structures and their vortical remnants, and that a tropical storm forms close to the center of the wave's gyre pouch via system-scale convergence in the lower troposphere and vorticity aggregation. Tory et al. recently adopted the Okubo-Weiss (OW) parameter to measure low-deformation vorticity in the marsupial pouch and suggested the importance of low-deformation vorticity in tropical cyclogenesis [11]. They found that most TCs that formed in tropical waves are associated with enhanced levels of the OW parameter at the 850 and 500 hPa pressure levels for at least 24 h prior to the time of TC declaration.

In fact, the role of low-deformation vorticity was noticed in terms of the Rossby radius of deformation in early studies, which suggested that the effective conversion of convective heating to storm-scale kinetic energy requires a substantial reduction in the Rossby radius of deformation to prevent convective heating being diffused away by gravity waves during the TC genesis (Schubert et al.[31]; Schubert and Hack [32]; Ooyama [3]; Simpson et al.[33]) also suggested that the low-deformation vorticity area may be necessary for the efficient conversion of convective heating to kinetic energy for system-scale intensification during tropical cyclogenesis. In this study, the role of tropical cyclogenesis precursors in establishing low-deformation vorticity areas is demonstrated by examining the WNP TC formation processes from the period 11 August to 10 September 2004. Further observational evidence is provided to confirm the role of synoptic-scale tropical disturbances associated with wave trains in the western North Pacific (WNP) monsoon trough in establishing the marsupial pouch for tropical cyclogenesis.

2 DATA AND METHODOLOGY

In this study tropical cyclogenesis precursors are identified using the wind data from the National Aeronautics and Space Administration (NASA) Modern Era Reanalysis for Research and Applications (MERRA) with a horizontal resolution of 1/2° latitude× 2/3° longitude at 42 vertical levels (Rienecker et al.[34]). Note that the MERRA assimilation system did not use the tropical storm relocation and bogus techniques (Lee et al.[35]). Although observations are continuously assimilated in the MERRA system, the TC centers are not necessarily coincident with the records in the Joint Typhoon Warning Center (JTWC) best track dataset. For this reason, a variational approach is used to locate TC centers in MERRA data (Wu et al.[36]).

In order to distinguish the contributions of the multi-scale circulations, a monsoon trough is treated as the low-frequency background relative to synoptic-scale flows such as tropical disturbances and TCs(Wu et al.[37, 38]) and a Lanczos time filter is used to obtain the low-frequency and synoptic-scale components from the MERRA data at each grid point (Lanczos[39]; Duchon[40]). Since Hsu et al. showed that TC circulation can significantly contribute to low-frequency variance on the intraseasonal time scale [41], the TC circulation is first removed from the MERRA data using the method proposed by Kurihara et al.[42, 43], and then a 10-day low-pass filter is applied to obtain the low-frequency background field. Previous studies indicate that the periods of synoptic disturbances can be 3–5 days and 6–10 days (Takayabu and Nitta[21]; Lau and Lau[20]). We conducted a spectral analysis of the relative vorticity in the monsoon trough and found two significant spectral peaks around 4 days and 8 days during the period 11 August to 10 September 2004 (figure not shown). Thus a band-pass filter with a cut-off period of 2–10 days is used to obtain the synoptic-scale components in this study.

3 TROPICAL CYCLOGENESIS

In this study, we take tropical cyclogenesis as a process by which a synoptic-scale disturbance intensifies first to the tropical depression strength (21 kt) and then to the tropical storm strength (35 kt) in the JTWC best track dataset. The genesis time is defined when a tropical disturbance first reached the tropical depression strength. Fig.1 shows the genesis time and subsequent tracks of the five TCs observed during the period 11 August – 10 September 2004. An 850-hPa low-pass filtered wind field averaged over this period is also plotted to show the locations of the monsoon trough and the subtropical high. Five TCs formed in the monsoon trough and generally took a northwestward track within the MT. During their late lifetime, Typhoon Aere moved southwestward and others recurved northward along the west boundary of the subtropical high.

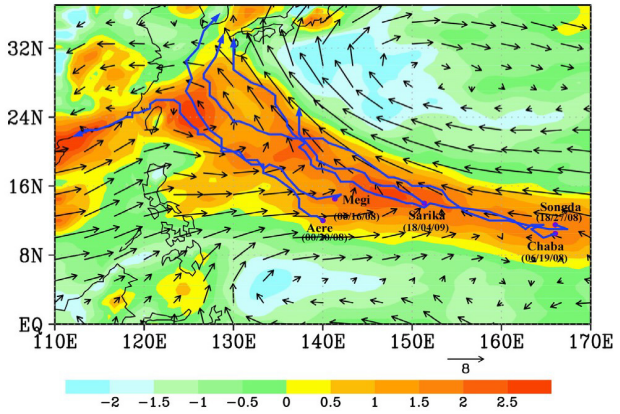

Figure 1. The 31-day time mean 850 hPa 10-day low-pass filtered winds (vector; m s^{-1}) and relative vorticity (shaded; 10^{-5} s^{-1}) superimposed with the track of tropical cyclones. Purple dots indicate the formation locations. Dates indicate the tropical cyclones formation time.

The evolution of the monsoon trough during 11 August–10 September 2004 can be seen in Fig.2a, in which the eastward extension (westward withdrawal) of the monsoon trough can be seen by the zero contour of the low-frequency 850-hPa zonal wind averaged over 3–15°N. Since 11 August the monsoon trough persistently extended eastward and reached its easternmost position around 170°E on 26 August, and then it retreated westward. Four of the TC genesis events occurred during the eastward extension of the monsoon trough, and one took place during the westward withdrawal. Typhoons Megi and Aere formed within the westerly region while the other three TCs formed near the shear line between the westerly wind and easterly wind.

The synoptic-scale 850-hPa wind fields associated with the five TC genesis events are shown in Fig.3. The synoptic-scale disturbances can be identified as cyclonic circulation of northwestward-propagating wave trains during the genesis of the five TCs. A tropical depression was named Megi at 1800 UTC on 13 August 2004 (Fig.3a), and it was upgraded to a tropical storm at 0600 UTC on 16 August. As the wave train moved northwestward along the monsoon trough line, tropical depression Chaba was first observed at 0600 UTC 18 August and developed into a tropical storm at 0600 UTC 19 August. Unlike the other four TCs, Chaba formed to the north of the anticyclonic circulation of the wave train (Fig.3b).

Tropical depression Aere was first detected at 0000 UTC on 19 August (Fig.3b) and reached the tropical storm strength at 0000 UTC on 20 August. Tropical depression Songda formed at 0000 UTC on 27 August 2004 (Fig.3c) and it became a tropical storm at 1800 UTC on 27 August. The genesis of Songda occurred when the monsoon trough reached its easternmost location during the period (Fig.2). When the wave train propagated northwestward in the monsoon trough,

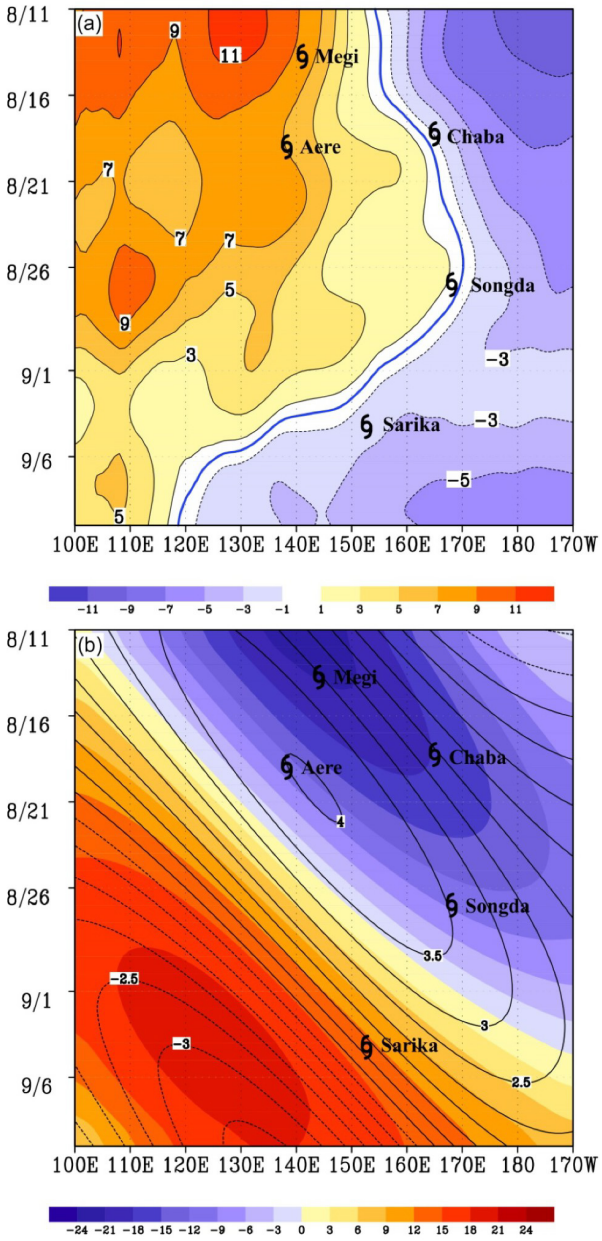

Figure 2. Longitude-time diagram of (a) the 850 hPa 10-day lowpass filtered zonal winds (shaded and contour; m s^{-1}) averaged 3°–15°N and (b) The MJO OLR anomalies (shaded; W m^{-2}) and the 850 hPa zonal wind (contour; m s^{-1}) along 10 °N superimposed with the longitudinal formation position of tropical cyclones during 11 August to 10 September 2004. The blue line indicates the low-frequency zero zonal wind.

another new cyclonic disturbance developed and the genesis of Sarika occurred in the cyclonic circulation at 0600 UTC 4 September (Fig.3d). Except Chaba, as shown in Fig.3, all of the other four tropical cyclogenesis events occurred in the cyclonic circulation of the wave train.

4 LOW–DEFORMATION VORTICITY AREAS

Following Tory et al.[11], the OW parameter is used to quantify the low-deformation vorticity, which is defined as follows (Okubo[44]; Weiss[45]; Rozoff et al.[46]),

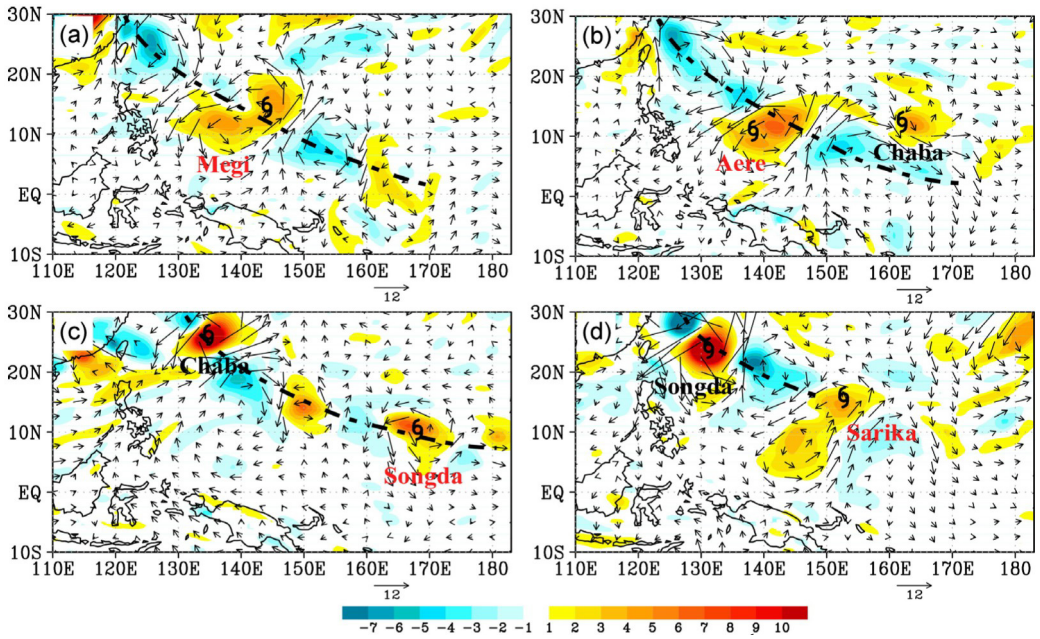

Figure 3. The 850 hPa 2-10-day bandpass filtered synoptic-scale wind fields (vector; m s^{-1}) and relative vorticity (shaded; 10^{-5} s^{-1}) at (a) 1800 UTC 13 August 2004, (b) 0000 UTC 19 August 2004, (c) 0000 UTC 27 August 2004, and (d) 0600 UTC 4 September 2004. The bold dashed lines indicate the monsoon trough lines.

$$OW=\zeta^2-(E^2+F^2)=\left(\frac{\partial v}{\partial x}-\frac{\partial u}{\partial y}\right)^2-\left(\frac{\partial u}{\partial x}-\frac{\partial v}{\partial y}\right)^2-\left(\frac{\partial v}{\partial x}+\frac{\partial u}{\partial y}\right)^2$$

where ζ is relative vorticity and E and F are the stretching deformation and shearing deformation, respectively. When the pure deformation terms are subtracted in relative vorticity, positive (negative) values of the OW parameter indicate the dominance of the rotation (deformation) in the flow.

Using a hypothetical tangential wind profile, Tory et al. (2013) found that the maximum OW is not located at the TC center [11]. We examined the spatial OW distribution for the wind profiles in Carr and Elsberry [47] and Mallen et al.[48]. Except the wind profile used by Carr and Elsberry [47], which shows a radial distribution of the OW parameter similar to that in Tory et al.[11], all of the wind profiles in Mallen et al. (2005) have the maximum OW at the TC center[48].

In order to further demonstrate the radial distribution of the OW, we use the multiplatform TC surface wind analysis (MTCSWA) product (Knaff et al. [49]). The MTCSWA is produced through multiple satellite wind data fusion algorithm by NOAA/NESDIS (http://www.ssd.noaa.gov/PS/TROP/mtcswa.html), covering global TCs at the sea surface (10 m) and flight-level (700 hPa). The advantage of the TC wind product is the relatively high horizontal resolution (0.1° latitude by 0.1° longitude) at 6-hour intervals. Fig.4 shows an example of the radial distribution of the OW parameter for observed TCs. The figure indicates that the maximum OW occurred at the center of Haiyan (2013) when it reached tropical depression, tropical storm and typhoon strengths. The positive OW

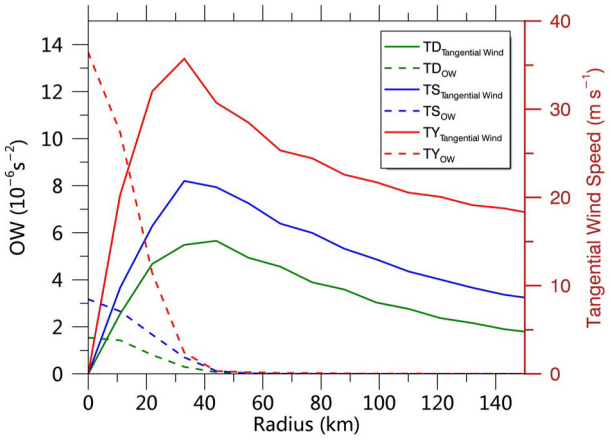

Figure 4. Radial profiles of azimuthal mean tangential wind (m s^{-1}) and Okubo-Weiss parameter (10^{-6} s^{-2}) at the center of Haiyan (2013) when it reached tropical depression (green), tropical storm (blue) and typhoon (red) strengths.

disappears immediately outside of the radius of maximum wind.

Figures 5 and 6 show the 850-hPa wind fields of the tropical cyclogenesis precursors and the associated OW fields for the TC genesis events of Megi and Chaba. The area of the low-deformation vorticity or positive OW associated with a genesis event is identified by tracking the disturbances backward from the genesis time since the TC center records are available in the JTWC best track data. In these figures, the time is indicated relative to the TC genesis time

(reaching the tropical depression strength) and the first and last panels indicate the OW fields when the positive OW area associated with the genesis is first detectable and the system reached tropical storm intensity, respectively. We can see that the positive OW is located in the tropical disturbances generally within a radius of about 500 km.

The positive OW area associated with the genesis of Megi is first detectable 60 hours prior to the genesis time (Fig.5a). Two maximum OW centers can be identified with a dominant one close to the enhanced southwest winds in the east side of the disturbance. Since a concentrated OW area means the flow with high rotation, the mesoscale circulations associated with the two maximum OW centers may interact with each other, but the interaction is hardly examined with the relatively coarse horizontal and temporal resolutions of the MERRA data. Although the positive OW area was still within the tropical disturbance 24 hours later (Fig. 5b), it shifted northwestward with the synoptic system and the rotation weakened as indicated by the decreased OW. At the genesis time (Fig.5c), the two OW maximum centers became a single one and the rotation in the central area is remarkably enhanced. As the disturbance continued to propagate northwestward, the concentrated low-deformation vorticity area was limited within a radius of about 300 km and the OW maximum center is coincident with the TC center (Fig.5d).

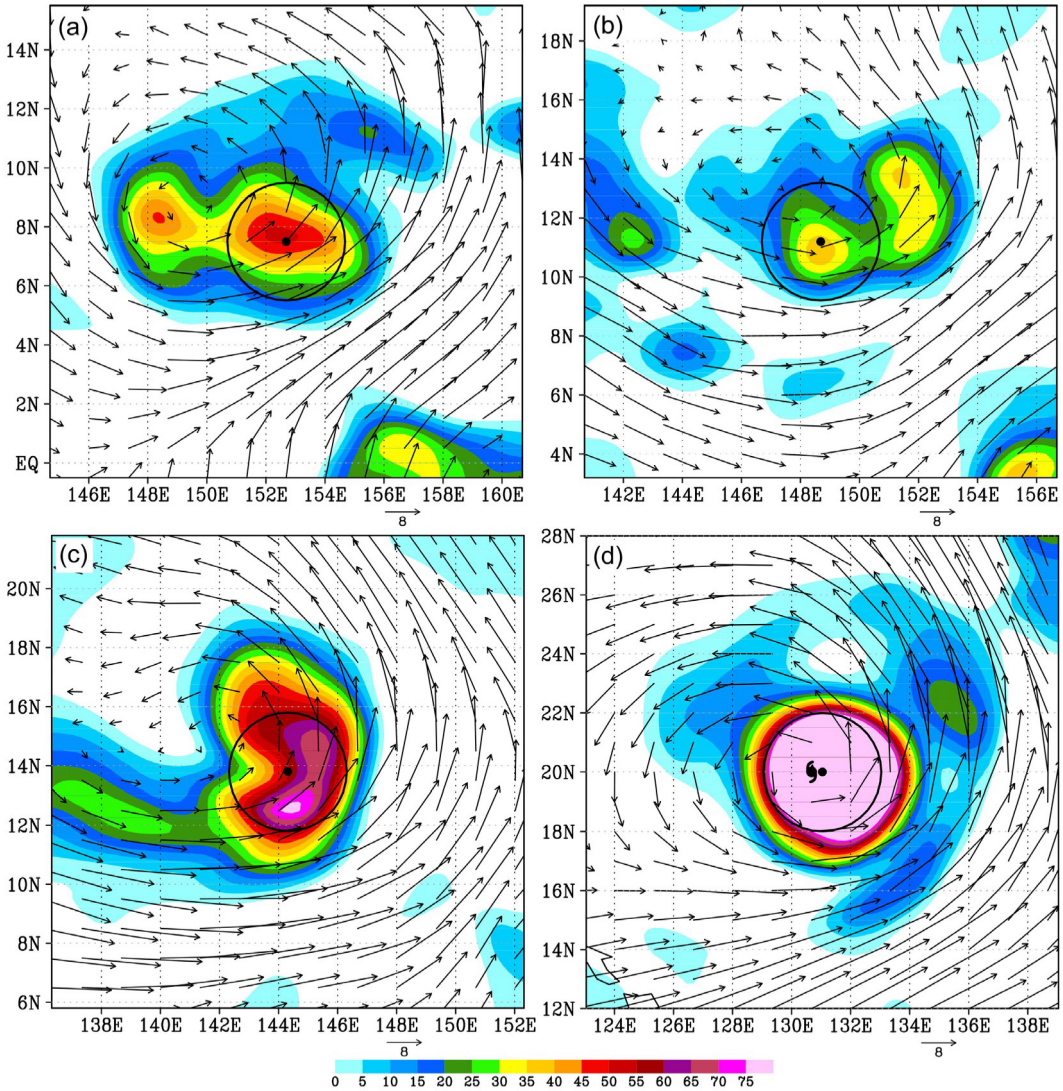

Figure 5. The 850 hPa wind fields (vector; m s^{-1}) and Okubo-Weiss parameter (shaded; 10^{-10} s^{-2}) at (a) -60 h, (b) -36 h, (c) 0 h, and (d) +60 h, with dots indicating the positive maximum OW center. The circles indicate the radius of 220 km away from the center. The typhoon mark indicates the tropical disturbance center associated with which Typhoon Megi.

The other four genesis events are similar to the genesis of Typhoon Megi in terms of the OW evolution. The concentrated positive OW areas can be clearly identified in the genesis events of Chaba, Aere, Songda and Sarika and the low-deformation area can be traced back 18–72 hours prior to the genesis time. Fig.6 shows an example for Typhoon Chaba. The positive OW increased during the TC genesis and was mainly

confined to an area with a radius of about 400 km. When the TCs intensified into a tropical storm, the OW maximum center is nearly collocated with the TC center. Figs.5 and 6 suggest that tropical cyclogenesis is accompanied with the enhancement of low-deformation vorticity in a limited area, mainly within a radius of 400–500 km, which is the favorable area for tropical cyclogenesis.

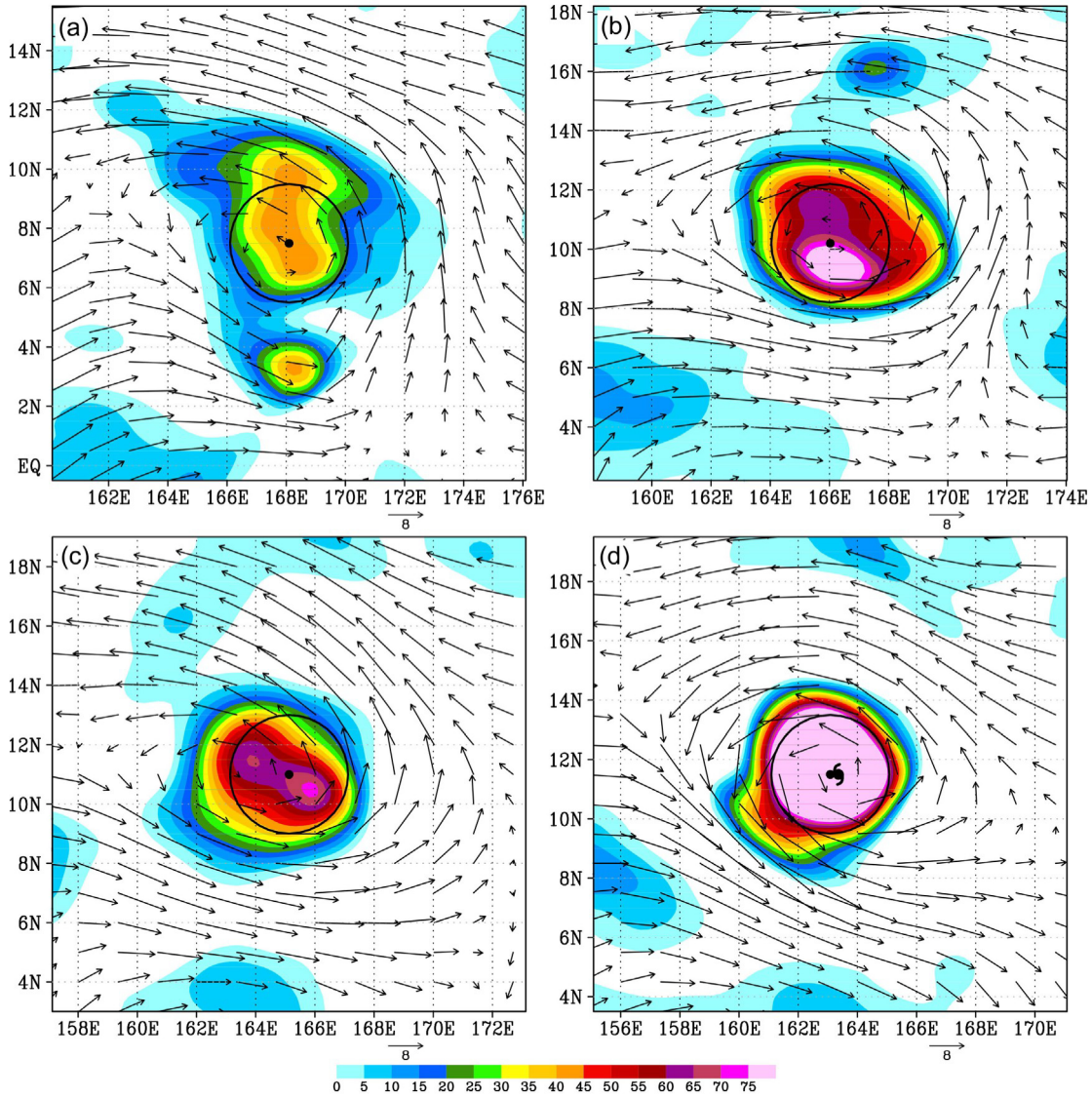

Figure 6. Same as Fig.5, but for Chaba at (a) −18 h, (b) 0 h, (c) +12 h, and (d) +24 h.

Figure 7 shows the vertical profiles of the OW parameter for the five tropical cyclogenesis events, which were calculated with the low-frequency and synoptic flows and averaged over the concentrated positive OW areas. We can see two features in this figure. First, the synoptic-scale OW is dominant compared to the low-frequency one, indicating that the low-deformation vorticity or high rotation in the favorable area of tropical cyclogenesis results mainly from the synoptic disturbance. Second, the low-deformation vorticity associated with the synoptic disturbance is located mainly in the low troposphere with a maximum between 700 and 900 hPa even when the concentrated positive OW area is initially detected (dashed lines in Fig.7). This figure suggests that the tropical cyclogenesis events were initially in the low levels, in agreement with Tory et al. (2013).

The evolution of the 850 hPa relative vorticity, OW and the two deformation terms indicates that the increasing relative vorticity results mainly from the rotational component while the two deformation terms remain nearly unchanged during TC genesis (Fig.8). It should be noted that the OW shows substantial variations with time, which may be associated with convective activity since the rotation in the marsupial pouch intensifies through vorticity aggregation associated with mesoscale convective systems (Montgomery et al.[30]).

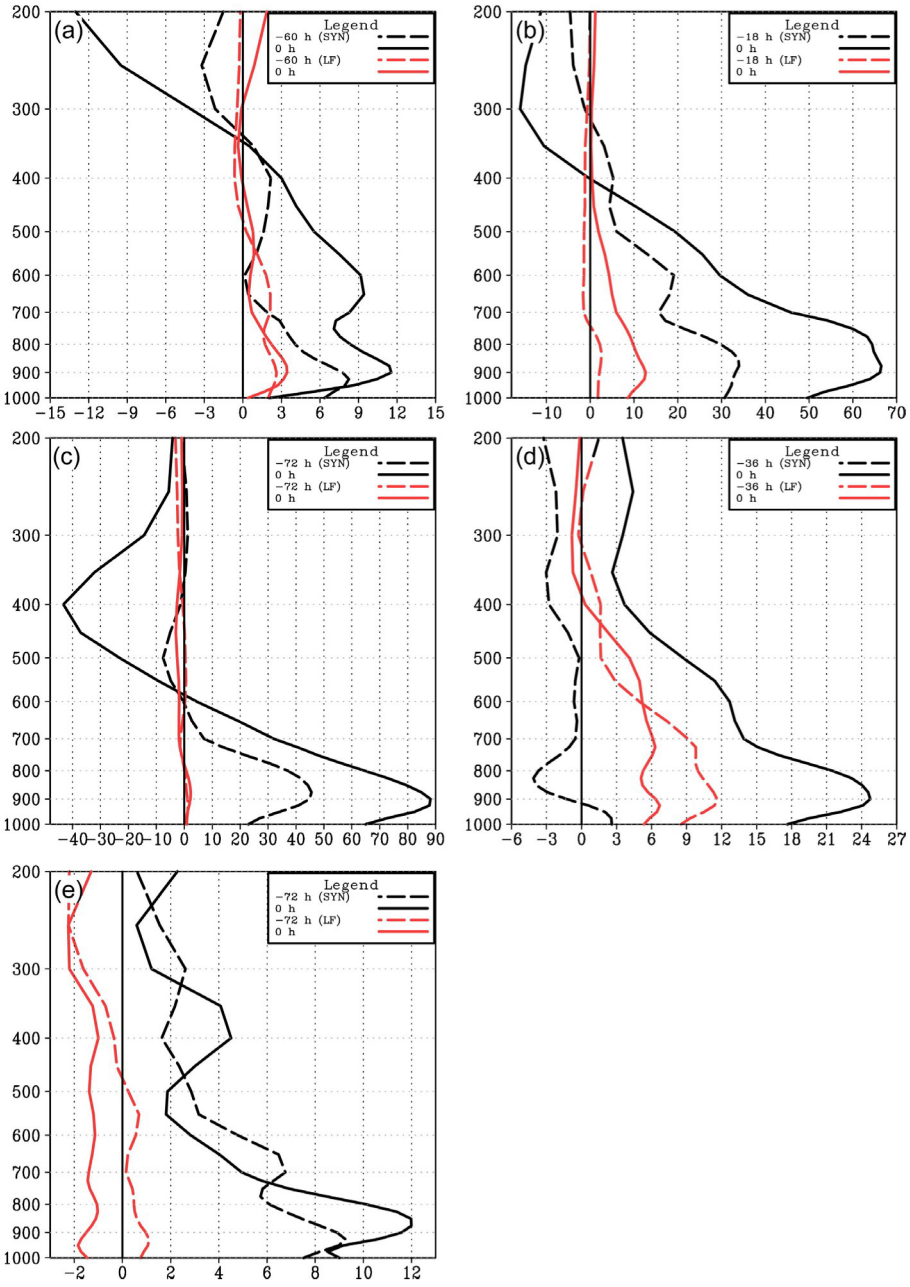

Figure 7. Vertical profiles of the regional averages of the Okubo-Weiss parameter (10^{-10} s^{-2}) of the synoptic-scale (SYN) and low-frequency (LF) flows within the circular central area of a 220-km radius from 1,000 hPa to 200 hPa.

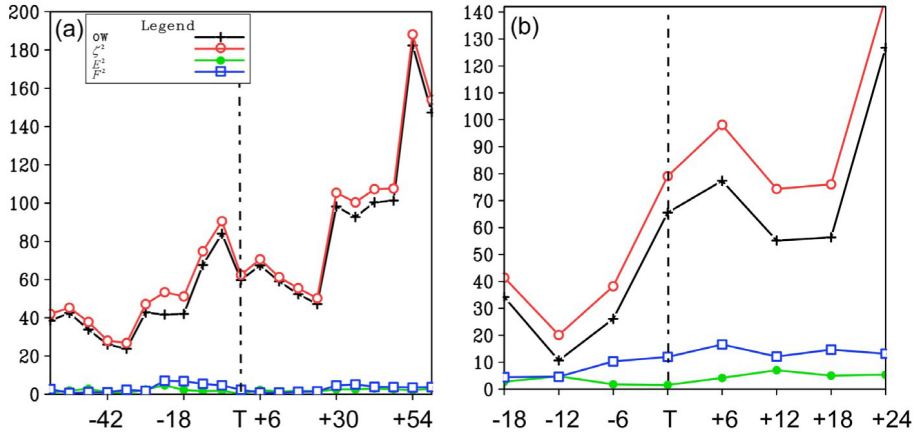

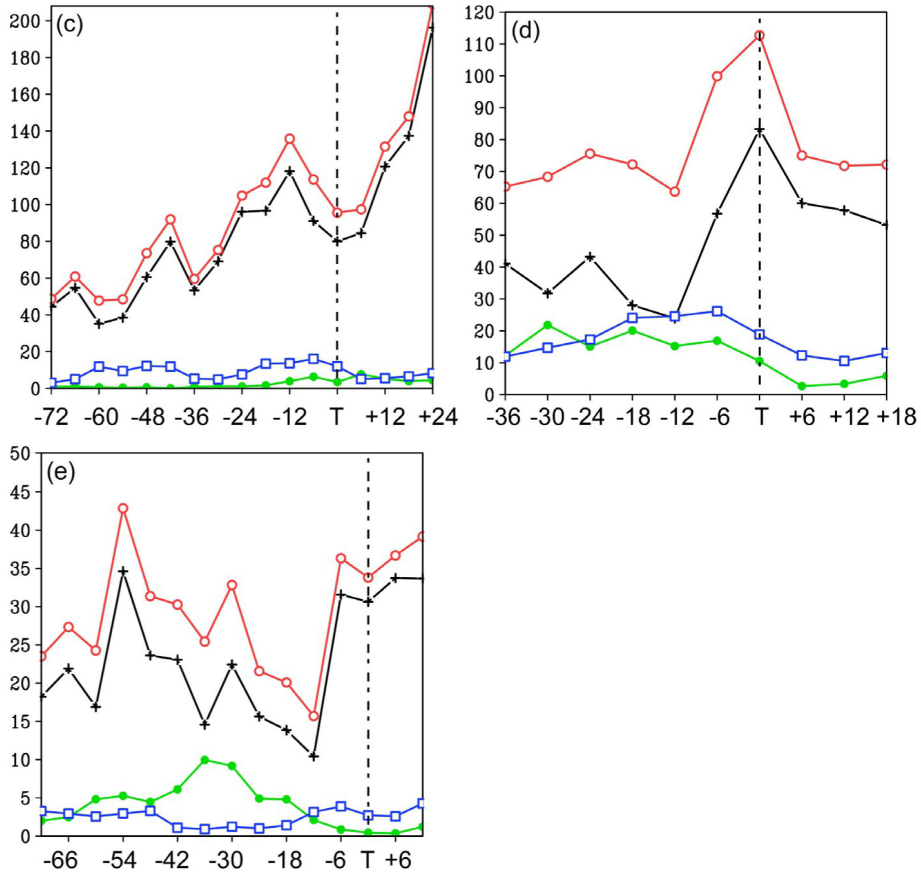

Figure 8. The 850 hPa relative vorticity (10^{-10} s^{-2}), Okubo-Weiss parameter (10^{-10} s^{-2}) and the two deformation terms (10^{-10} s^{-2}).

5 DISCUSSION

Since previous studies suggested that the Rossby radius of deformation should be decreased to enable convective heating to convert into storm-scale kinetic energy (Schubert et al.[31]; Schubert and Hack[32]; Gill[50]; Ooyama [3]; Simpson et al.[33]), here we calculated the Rossby radius of deformation in the high-rotation area. In this study, the Rossby radius of deformation in the lower troposphere is estimated as $L_R=NH/\pi\eta$, where N, H and η are the static stability, the depth of the system and the absolute vorticity, respectively. As discussed in the last section, the low-deformation areas in the genesis events are confined mostly to the low-to-middle troposphere. For this reason, absolute vorticity η is averaged over the layer between 1,000 hPa and 500 hPa, and the depth of the system and the static stability are estimated as $H=R\bar{T}/g$ and $N=\sqrt{\frac{g}{\theta}\frac{d\theta}{dz}}$, where g and R are the gravitational constant and the gas constant for dry air, temperature $\bar{T}$ and the potential temperature are averaged over the layer 500 and 1,000 hPa, and $\frac{d\theta}{dz}$ is the difference of potential temperatures between 500 and 1,000 hPa.

Figure 9 shows the evolution of the Rossby radius of deformation during the genesis processes. The radii generally decrease in the low-deformation areas. The radius is generally about 600–800 km at the beginning of the genesis processes and reduced to 400–600 km when the systems reached the tropical depression strength. Since the Rossby radius of deformation is still larger than the horizontal scale of Mesoscale Convection Systems (MCSs, Gray[5]) or the low-deformation area, it is suggested that convective heating cannot be effectively converted into the kinentic energy of the low-deformation directly in the low-deformation area. That is, other processes should be involved in the development of the circulation in the low-deformation area. Our study shows that the low-deformation vorticity results mainly from synoptic disturbances, which provide a limited area for tropical cyclogenesis. Previous studies have pointed out that MCSs are always embedded in synoptic-scale disturbances with a horizontal scale of about 250 km. The MCS systems can establish an area of higher relative vorticity. The mesoscale circulations that interact with each other may be important for the development of the circulation in the low-deformation area, further reducing the Rossby radius of deformation, but this part is hardly examined with the relatively coarse horizontal and temporal resolutions of the MERRA data. Thus, the development of the circulation in the low-deformation area will be examined further by

conducting a series of numerical experiments with higher horizontal resolution.

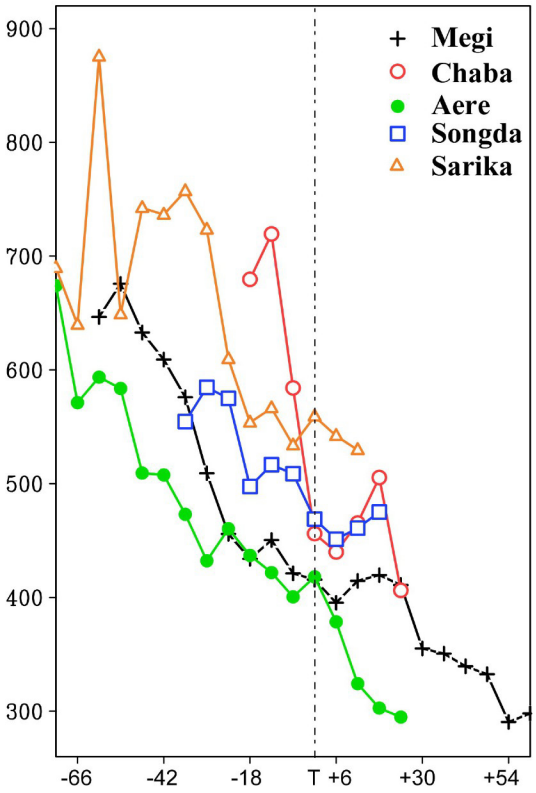

Figure 9. Time series of the Rossby radius of deformation calculated using 220 km by 220 km area-averaged data from the MERRA data. The vertical line denotes the time for the occurrence of tropical cyclogenesis.

A few mechanisms were proposed for the development of synoptic-scale wave trains, including Rossby wave energy dispersion of a preexisting TC (Holland [51]; Li et al.[52]; Li and Fu [53]; Li et al.[54]), transition of mixed Rossby-gravity (MRG) waves to off-equatorial tropical-depression-type (TD-type) waves (Takayabu and Nitta[21]; Liebmann and Hendon[55]; Dickinson and Molinari[56]; Aiyyer and Molinari[57]; Chen and Huang [58]), scale contraction and energy accumulation of equatorial waves (Tai and Ogura[59]; Holland[51]; Kuo et al.[60]; Sobel and Maloney[61]; Hartmann and Maloney [62]; Maloney and Hartmann[63]; Maloney and Dickinson [64]; Tam and Li [65]; Gall and Frank [66]), and instability of summer mean flows in the presence of a convection-frictional convergence (CFC) feedback (Li[67]).

Idealized numerical studies have been conducted on the influence of low-frequency background on the development of TC precursor disturbances. Aiyyer and Molinary examined the role of the idealized MJO flow in the growth of off-equatorial disturbances that were initiated by MRG waves in a shallow water model[57]. They found that the off-equatorial disturbance can develop by obtaining kinetic energy from the MJO flow, suggesting the importance of the MJO flow and MRG waves for the development of off-equatorial disturbances. To demonstrate the possible role of MRG waves, the wavenumber-frequency spectrum analysis is used to obtain the components of the MJO and equatorial waves in the MERRA analysis data within 20° of the equator (Wheeler and Kiladis[68]).

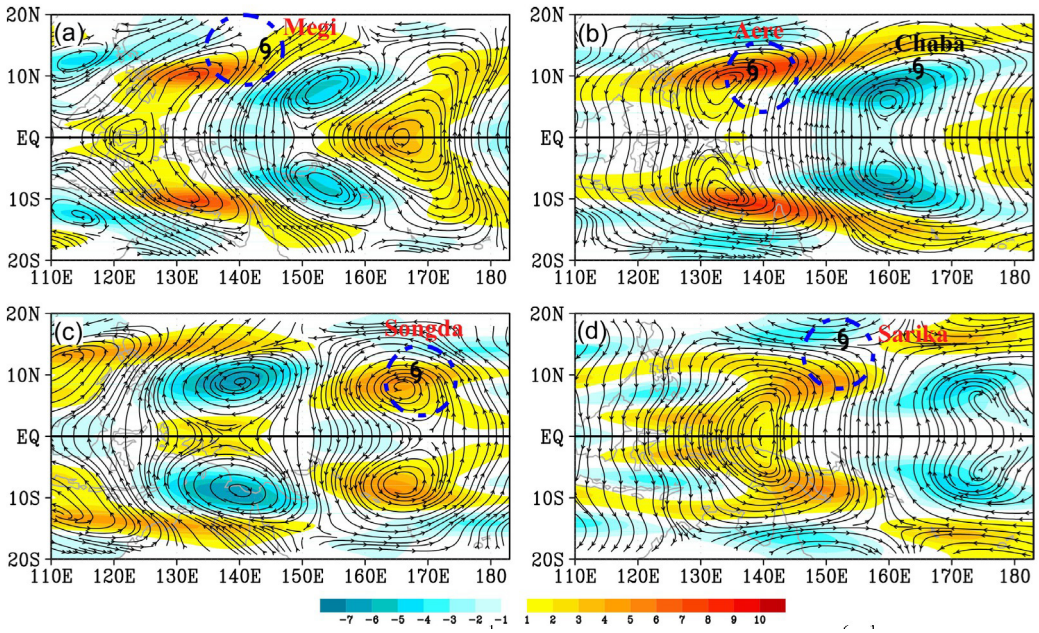

Figure 10. The 850 hPa MRG wave wind fields (stream; m s^{-1}) and relative vorticity (shaded; 10^{-6} s^{-1}) at (a) 1800 UTC 13 August 2004, (b) 0000 UTC 19 August 2004, (c) 0000 UTC 27 August 2004, and (d) 0600 UTC 4 September 2004.

Figure 2b shows the MJO component of zonal wind and OLR along 10 °N. Compared to Fig.2a, the eastward extension and westward withdrawal of the MT are closely related to the active (westerly wind and negative OLR anomalies) and inactive (easterly wind and positive OLR anomalies) periods of the MJO. During 11 – 28 August 2004, the westerly wind associated with the MJO extended eastward. During this period, the MT extended eastward and reached its easternmost position on 28 August. The westward withdrawal of the MT was coincident with the easterly phase of the MJO. As part of the background field, the MJO affects the monsoon trough and the monsoon trough further affects the development of synoptic-scale disturbances by other mechanism (e. g. kinetic energy conversion mechanism). Except the genesis of Chaba, we can also see that the tropical cyclogenesis was closely associated with the counterclockwise circulation of the MRG wave, which was centered at the equator around 135°E and extended in the northeast (southeast) direction in the Northern (Southern) Hemisphere at 1800 UTC 13 August (Fig.10a).

The features can also be seen in the genesis processes of Aere, Songda and Sarika. As Megi intensified and moved northwestward, the wave train pattern became very clear. The genesis of Aere was within the tropical disturbance at 0000 UTC 19 August, and also coupled with the counterclockwise circulation of the MRG wave (Fig.10b). The genesis of Songda occurred when the MT reached its easternmost location during the period (Fig.2). At 0000 UTC 27 August (Fig. 10c), the genesis location of Songda was within the counterclockwise circulation of MRG wave. Another new cyclonic disturbance developed near 160 °E at 0600 UTC 2 September, which was also coupled with the counterclockwise circulation of the MRG wave (figure not shown). As the disturbance moved westward, the genesis of Sarika occurred in the cyclonic circulation, but to the north of the counterclockwise circulation of the MRG wave (Fig.10d). It is indicated that the genesis events of Megi, Aere, Songda and Sarika occurred in the cyclonic circulation of the northwestward-propagating wave train, and the initial development of these cyclonic circulations or disturbances are well coupled with the counterclockwise circulation of the MRG wave. It is worthwhile to note that wind speeds of MRG waves are about 2 m/s and thus the role of MRG waves in providing the low-deformation vorticity areas is very limited.

6 SUMMARY

It has long been known that incipient tropical cyclones (TCs) always occur in synoptic-scale disturbances. Here the role of tropical cyclogenesis precursors in establishing low-deformation vorticity areas is examined through an analysis of tropical cyclogenesis events that occurred during 11 August to 10 September 2004. In this study, the low-frequency circulation obtained with a 10-day low-pass time filter is treated as the background of synoptic-scale disturbances and a band-pass time filter with a cut-off period of 2 – 10 days is used to separate the synoptic-scale component.

Our analysis of the five tropical cyclogenesis events shows that synoptic-scale tropical cyclogenesis precursors provide a region of low-deformation vorticity that is measured with the positive OW parameter. The OW concentrated areas are within the tropical cyclogenesis precursors with a radius of about 400–500 km and can be found as early as 72 hours prior to the formation of the tropical depression. When the TC reached the tropical storm intensity, the concentrated OW is confined to an area of 200–300 radius and the storm centers are coincident with the centers of the maximum OW. This study suggests that the tropical cyclogenesis occurs in the low-deformation area and can be identified 18 –72 hours prior to the formation of tropical depressions. The results confirm recent studies that low-deformation vorticity is important in TC formation and that the pre-existent synoptic-scale disturbances play an important role in establishing the area of low-deformation vorticity (Tory et al.[11]).

As expected in previous studies (Schubert et al.[31]; Schubert and Hack[32]; Ooyama[3]; Simpson et al. 1997[33]), our calculation indicates that the Rossby radius of deformation is reduced as TC genesis precedes, but the reduction does not sufficiently make the effective conversion of convective heating into the kinetic energy within the low-deformation area. It is suggested that other processes should be involved in the development of the circulation in the low-deformation area. In particular, we find that the initial development of four of these disturbances is coupled with the counterclockwise circulation of the MRG wave, in support of the role of MRG waves in tropical cyclogenesis (Takayabu and Nitta [21]; Liebmann and Hendon [55]; Dickinson and Molinari [56]; Aiyyer and Molinari[57]; Chen and Huang[58]).

REFERENCES:

[1] RIEHL H. On the formation of typhoons [J]. J Meteorol, 1948, 5: 247-265.
[2] RAMAGE C S. Hurricane development [J]. J Meteorol, 1959, 16: 227-237.
[3] OOYAMA K. Conceptual evolution of the theory and modeling of the tropical cyclone [J]. J Meteorol Soc Japan, 1982, 60: 369-379.
[4] ZEHR R M. Tropical cyclogenesis in the western North Pacific. NOAA Technical Report NESDIS [R]. NESDIS, Washington, DC, 1992, 16: 181.
[5] GRAY W M. The formation of tropical cyclones [J]. Meteorol Atmos Phys, 1998, 67: 37-69.
[6] DUNKERTON T J, MONTGOMERY M T, WANG Z. Tropical cyclogenesis in a tropical wave critical layer:

easterly waves [J]. Atmos Chem Phys, 2009, 9: 5587-5646.
[7] WAND Z, MONTGOMERY M T, DUNKERTON T J. Genesis of pre-Hurricane Felix (2007). Part II: Warm core formation, precipitation evolution, and predictability [J]. J Atmos Sci, 2009, 67: 1730-1744.
[8] MONTGOMERY M T, WANG Z, DUNKERTON T J. Intermediate and high resolution numerical simulations of the transition of a tropical wave critical layer to a tropical storm [J]. Atmos Chem Phys Discuss, 2009, 9: 26143-26197.
[9] MONTGOMERY M T, WANG Z, DUNKERTON T J. Coarse, intermediate and high resolution numerical simulations of the transition of a tropical wave critical layer to a tropical storm [J]. Atmos Chem & Physics, 2010, 10: 10803-10827.
[10] WANG Z, DUNKERTON T J, MONTGOMERY M T. Application of the marsupial paradigm to tropical cyclone formation from northwestward-propagating disturbances [J]. Mon Wea Rev, 2012, 140: 66-76.
[11] TORY K J, DARE R A, DAVIDSON N E, et al. The importance of low-deformation vorticity in tropical cyclone formation [J]. Atmos Chem Phys, 2013, 13: 2115-2132.
[12] SADLER J C. Average Monthly Cloud Coverage of the Global Tropics Determined from Satellite Observations [R]. Proc of the Working Panel on Tropical Dynamic Meteorology, Monterey, Calif Navy Weather Research Facility Report No. 12-1167-132. 1967. pp: 155-163.
[13] SADLER J C. The monsoon circulation and cloudiness over the GATE area [J]. Mon Wea Rev, 1975, 103: 369-387.
[14] GRAY W M. Global view of the origins of tropical disturbances and storms [J]. Mon Wea Rev, 1968, 96: 669-700.
[15] GRAY W M. Tropical cyclone genesis [R]. Dept of Atmos Sci Paper No 234, Colo. State Univ, Ft Collins, CO. 1975, pp: 121.
[16] FRANK W M. Tropical cyclone formation (Chapter 3) [M]// A Global View of Tropical Cyclones, WMO Bangkok, Thailand textbook, Printed by Dept of Chicago, 1987, 53-90.
[17] CHEN T C, WANG S Y, YEN M C. Interannual variation of the tropical cyclone activity over the western North Pacific [J]. J Climate, 2006, 19: 5709-5720.
[18] CHEN T C, WENG S P, YAMAZAKI N, et al. Interannual variation in the tropical cyclone formation over the western North Pacific [J]. Mon Wea Rev, 1998, 126: 1080-1090.
[19] NITTA T. On the role of transient eddies in the tropical troposphere [J]. J Meteorol Soc Japan , 1970, 48: 348-359.
[20] LAU K H, LAU N C. Observed structure and propagation characteristics of tropical summertime synoptic scale disturbances [J]. Mon Wea Rev, 1990, 118: 1888-1913.
[21] TAKAYABU Y N, NITTA T. 3-5 day period disturbances coupled with convection over the tropical Pacific Ocean [J]. J Meteorol Soc Japan, 1993, 71: 221-245.
[22] CHANG C P, CHEN J, HARR P, et al. Northwestward propagating wave patterns over the tropical western North Pacific during summer [J]. Mon Wea Rev, 1996, 124: 2245-2266.
[23] SOBEL A H, BRETHERTON C S. Development of synoptic-scale disturbances over the summertime tropical northwest Pacific [J]. J Atmos Sci, 1999, 56: 3106-3127.
[24] ZEHR R M. Tropical cyclone intensification [R]. Dept of Atmos Sci Paper No 259, Colo. State Univ, Ft Collins, CO. 1976, pp: 91 .
[25] MCBRIDE J L, ZEHR R. Observational analysis of tropical cyclone formation. Part II: Comparison of non-developing versus developing systems [J]. J Atmos Sci, 1981, 38: 1132-1151.
[26] LEE C S. Observational analysis of tropical cyclogenesis in the western North Pacific. Part I: Structural evolution of cloud clusters [J]. J Atmos Sci, 1989, 46: 2580-2598.
[27] FU B, PENG M S, LIT, et al. Developing versus nondeveloping disturbances for tropical cyclone formation. Part II: western North Pacific [J]. Mon Wea Rev, 2012, 140: 1067-1080.
[28] WANG Z, MONTGOMERY M T, DUNKERTON T J. Genesis of pre-Hurricane Felix (2007). Part I: The role of the easterly wave critical layer [J]. J Atmos Sci, 2010a, 67: 1711-1729.
[29] WANG Z, MONTGOMERY M T, DUNKERTON T J. Genesis of pre-Hurricane Felix (2007). Part II: Warm core formation, precipitation evolution, and predictability [J]. J Atmos Sci, 2010b, 67: 1730-1744.
[30] MONTGOMERY M T, LUSSIER III L L, MOORE R W, et al. The genesis of typhoon Nuri as observed during the tropical cyclone structure 2008 (TCS-08) field experiment—Part 1: The role of the easterly wave critical layer [J]. Atmos Chem Phys, 2010a, 10: 9879-9900.
[31] SCHUBERT W H, HACK J J, DIAS P L S, et al. Geostrophic adjustment in an axisymmetric vortex [J]. J Atmos Sci, 1980, 37: 1464-1484.
[32] SCHUBERT W H, HACK J J. Inertial stability and tropical cyclone development [J]. J Atmos Sci, 1982, 39: 1687-1697.
[33] SIMPSON J, RITCHIE E, HOLLAND G J, et al. Mesoscale interactions in tropical cyclone genesis [J]. Mon Wea Rev, 1997, 125: 2643-2661.
[34] RIENECKER M M, SUAREZ M J, GELARO R, et al. MERRA: NASA's Modern-Era Retrospective Analysis for Research and Applications [J]. J Climate, 2011, 24: 3624-3648.
[35] LEE M L, SCHUBERT S D, KIM D. Representation of tropical storms in the Northwestern Pacific by the Modern-Era Retrospective analysis for research and applications [J]. Asia-Pacific J Atmos Sci, 2011, 47(3): 245-253.
[36] WU L, BRAUN S A, HALVERSON J, et al. A numerical study of hurricane Erin (2001). Part I: Model verification and storm evolution [J]. J Atmos Sci, 2006, 63: 65-86.
[37] WU L, ZONG H, LIANG J. Observational analysis of tropical cyclone formation associated with monsoon gyres [J]. J Atmos Sci, 2013, 70: 1023-1034.
[38] WU L, NI Z, DUAN J, et al. Sudden tropical cyclone track changes over the western North Pacific: A composite study [J]. Mon Wea Rev, 2013, 141: 2597-2610.
[39] LANCZOS C. Applied analysis [M]. Prentice Hall, 1956, pp: 539.
[40] DUCHON C E. Lanczos filtering in one and two dimensions [J]. J Appl Meteorol, 1979, 8: 1016-1022.

[41] HSU H H, HUNG C H, LO A K, et al. Influence of tropical cyclones on the estimation of climate variability in the tropical western North Pacific [J]. J Climate, 2008, 21: 2960-2975.
[42] KURIHARA Y, BENDER M A, TULEYA R E, et al. An initialization scheme of hurricane models by vortex specification [J]. Mon Wea Rev, 1993, 121: 2030-2045.
[43] KURIHARA Y, BENDER M A, TULEYA R E, et al. Improvements in the GFDL hurricane prediction system [J]. Mon Wea Rev, 1995, 123: 2791-2801.
[44] OKUBO A. Horizontal dispersion of floatable particles in the vicinity of velocity singularities such as convergences [J]. Deep Sea Res, 1970, 17: 445-454,.
[45] WEISS J. The dynamics of enstrophy transfer in two-dimensional hydrodynamics [J]. Phys D, 1991, 48: 273-294.
[46] ROZOFF C, SCHUBERT W, BRIAN D, et al. Rapid filamentation zones in intense tropical cyclones [J]. J Atmos Sci, 2006, 63: 325-340.
[47] CARR L E, ELSBERRY R L. Monsoonal interactions leading to sudden tropical cyclone track changes [J]. Mon Wea Rev, 1995, 123: 265-290.
[48] MALLEN K J, MONTGOMERY M T, WANG B. Reexamining the near-core radial structure of the tropical cyclone primary circulation: implications for vortex resiliency [J]. J Atmos Sci, 2005, 62: 408-425.
[49] KNAFF J A, DEMARIA M, MOLENAR D A. An automated, objective, multiple-satellite-platform tropical cyclone surface wind analysis [J]. J Appl Meteorol Climatol, 2011, 50: 2149-2166.
[50] GILL A E. Atmosphere-Ocean Dynamics [M]. Academic Press, Orlando, 1982, pp: 662 .
[51] HOLLAND G J. Scale interaction in the Western Pacific Monsoon [J]. Meteorol Atmos Phys, 1995, 56: 57-79.
[52] LI T, FU B, GE X, et al. Satellite data analysis and numerical simulation of tropical cyclone formation [J]. Geophys Res Lett, 2003, 30: 2122, doi: 10.1029/2003GL018556.
[53] LI T, FU B. Tropical cyclogenesis associated with Rossby wave energy dispersion of a preexisting typhoon. Part I: Satellite data analyses [J]. J Atmos Sci, 2006, 63: 1377-1389.
[54] LI T, GE X, WANG B, et al. Tropical cyclogenesis associated with Rossby wave energy dispersion of a preexisting typhoon. Part II: Numerical simulations [J]. J Atmos Sci, 2006, 63: 1390-1409.
[55] LIEBMANN B, HENDON H H. Synoptic-scale disturbances near the equator [J]. J Atmos Sci, 1990, 47: 1463-1479.
[56] DICKINSON M, MOLINARI J. Mixed Rossby-Gravity waves and western Pacific tropical cyclogenesis. Part I: Synoptic evolution [J]. J Atmos Sci, 2002: 59: 2183-2196.
[57] AIYYER A, MOLINARI J. Evolution of mixed Rossby-gravity waves in idealized MJO environments [J]. J Atmos Sci, 2003, 60: 2837-2855.
[58] CHEN G H, HUANG R H. Interannual variations in mixed Rossby-Gravity waves and their impacts on tropical cyclogenesis over the western North Pacific [J]. J Climate, 2009, 22: 535-549.
[59] TAI K S, OGURA Y. An observational study of easterly waves over the eastern Pacific in the northern summer using FGGE data [J]. J Atmos Sci, 1987, 44: 339-361.
[60] KUO H C, CHEN J H, WILLIAMS R T, et al. Rossby waves in zonally opposing mean flow: Behavior in northwest Pacific summer monsoon [J]. J Atmos Sci, 2001, 58: 1035-1050.
[61] SOBEL A H, MALONEY E D. Effect of ENSO and the MJO on western North Pacific tropical cyclones [J]. Geophys Res Lett, 2000, 27(12): 1739-1742.
[62] HARTMANN D L, MALONEY E D. The Madden-Julian Oscillation, barotropic dynamics, and north Pacific tropical cyclone formation. Part II: Stochastic barotropic modeling [J]. J Atmos Sci, 2001, 58: 2559-2570.
[63] MALONEY E D, HARTMANN D L. The Madden-Julian Oscillation, barotropic dynamics, and North Pacific tropical cyclone formation. Part I: Observations [J]. J Atmos Sci, 2001, 58: 2545-2558.
[64] MALONEY E D, DICKINSON M J. The Intraseasonal Oscillation and the energetics of summertime tropical western North Pacific synoptic-Scale disturbances [J]. J Atmos Sci, 2003, 60: 2153-2168.
[65] TAM C Y, LI T. The origin and dispersion characteristics of the observed tropical summertime synoptic-scale waves over the Western Pacific [J]. Mon Wea Rev, 2006, 134: 1630-1646.
[66] GALL J S, FRANK W M. The role of equatorial Rossby waves in tropical cyclogenesis. Part II: Idealized simulations in a monsoon trough environment [J]. Mon Wea Rev, 2010, 138: 1383-1398.
[67] LI T. Origin of the summertime synoptic-scale wave train in the western north pacific [J]. J Atmos Sci, 2006, 63: 1093-1102.
[68] WHEELER M, KILADIS G N. Convectively coupled quatorial waves: Analysis of clouds and temperature in the wavenumber-frequency domain [J]. J Atmos Sci, 1999, 56: 374-399.

Citation: DUAN Jing-jing and WU Li-guan. Low-deformation vorticity areas in synoptic-scale disturbances for tropical cyclogenesis: An observational analysis [J]. J Trop Meteorol, 2017, 23(2): 121-132.